



.....

DESIGN AND SIMULATION ANALYSIS OF OUTER STATOR INNER ROTOR DFIG BY 2D AND 3D FINITE ELEMENT METHODS

H. Mellah^{‡*}, K. E. Hemsas^{*}

LAS, Laboratoire d'Automatique de Sétif, Department of Electrical Engineering, Sétif 1 university, Sétif,
Algeria.

[‡]Corresponding Author; Mellah Hacem, Department of electrical engineering, Faculty of Technologie University
Ferhat Abbas of Setif, Cité Maabouda, Route de Béjaia / 19000 / Algérie, 213 05 53 03 87 39,
mell_has@yahoo.fr

Abstract

In this paper, a time stepping 2D and 3D FEM is performed for modeling and analysis interior rotor DFIG. The finite element method currently represents the state-of-the-art in the numerical magnetic field computation relating to electrical machines. FEM is a numerical method to solve the partial differential equations (PDE) that expresses the physical quantities of interest, in this case Maxwell's equations. This will result in a more accurate result compared to analytical modeling, which can be regarded as a simplification of the PDE. FEM analysis is used for transient mode, magnetic field calculation, the magnetic flux density and vector potential of machine is obtained. In this model we including, non linear material characteristics, eddy current effect, torque-speed characteristics, ambient temperature effect and magnetic analysis are investigated.

Keywords- Modelling, DFIG, FEM, Wind Turbines, Energy.

1. Introduction

There is now general acceptance that the burning of fossil fuels is having a significant influence on the global climate. Effective mitigation of climate change will require deep reductions in greenhouse gas emissions, with UK estimates of a 60–80% cut being necessary by 2050 [1], Still purer with the nuclear power, this last leaves behind dangerous wastes for thousands of years and risks contamination of land, air, and water[2]; the catastrophe of Japan is not far. Wind power can contribute to fulfilling several of the national environmental quality objectives decided by Parliament in 1991. Continued expansion of wind power is therefore of strategic importance [3], hence, the energy policy decision states that the objective is to facilitate a change to an ecologically sustainable energy production system [3], as example the Swedish Parliament adopted new energy guidelines in 1997 following the trend of moving towards an ecologically sustainable society. The decision also confirmed that

the 1980 and 1991 guidelines still apply, i.e., that the nuclear power production is to be phased out at a slow rate so that the need for electrical can be met without risking employment and welfare. The first nuclear reactor of Barseback was shut down 30th of November 1999. Nuclear power production shall be replaced by improving the efficiency of electricity use, conversion to renewable forms of energy and other environmentally acceptable electricity production technologies [3]. On the individual scale in Denmark Poul la Cour, who was among the first to connect a windmill to a generator [4]. In real wind power market, three types of wind power system for large wind turbines exist. The first type is fixed-speed wind power (SCIG), directly connected to the grid. The second one is a variable speed wind system using a DFIG or SCIG. The third type is also a variable speed wind turbine, PMSG [5]. One can notice two problems of PMSG used in wind power. First is the inherent cogging torque due to magnet materials naturally attractive force. This kind of torque is bad for operation, especially stopping wind turbine starting and making noise and vibration in regular operation. The other one is the risk of demagnetization because of fault happening and overheating of magnets. This risk is very dangerous and the cost for replacing bad magnets is much higher than the generator itself [5]. There are several reasons for using variable-speed operation of wind turbines; the advantages are reduced mechanical stress and optimized power capture. Speed variability is possible due to the AC–DC–AC converter in the rotor circuit required to produce rotor voltage at slip frequency. Using a back-to-back converter allows bidirectional power flows and hence operation at both sub- and super-synchronous speeds. Formulating the control algorithm of the converters in a synchronously rotating frame allows for effective control of the generator speed (or active power) and terminal voltage [6]. Without forgotten the second major advantage of the DFIG, which has made it popular, is that the power electronic equipment only has to handle a fraction (20–30%) of the total system power [3]. This means that the losses in the power electronic equipment can be reduced in comparison to power electronic equipment that has to handle the total system power as for a direct-driven synchronous generator, apart from the cost saving of using a smaller converter.

2. Review of Related Research

The development of modern wind power conversion technology has been going on since 1970s, and the rapid development has been seen from 1990s. Various wind turbine concepts have been developed and different wind generators have been built [7]. The average annual growth rate of wind turbine installation is around 30% during last ten years [8].

At the end of 2006, the global wind electricity generating capacity increased to 74223 MW from 59091 MW in 2005. By the end of 2020, it is expected that this will have increased to well over 1260000 MW, which will be sufficient for 12% of the world's electricity consumption [7-8]. Fig. 1 depicts the total wind power installed capacity for some countries from 1985 to 2006. The countries with the highest total installed capacity are Germany (20 622 MW), Spain (11 615 MW), the USA (11 603 MW), India (6270 MW) and Denmark (3136 MW) [7-8].

In addition, the Global Wind Energy Council (GWEC) results, Europe continues to lead the market with 48,545 MW of installed capacity at the end of 2006, representing 65 % of the global total installation. The European Wind Energy Association (EWEA) has set a target of satisfying 23% European electricity needs with wind energy by 2030. It is clear that the global market for the electrical power produced by wind turbines has been increasing steadily, which directly pushes the wind generation technology into a more competitive area [8-7].

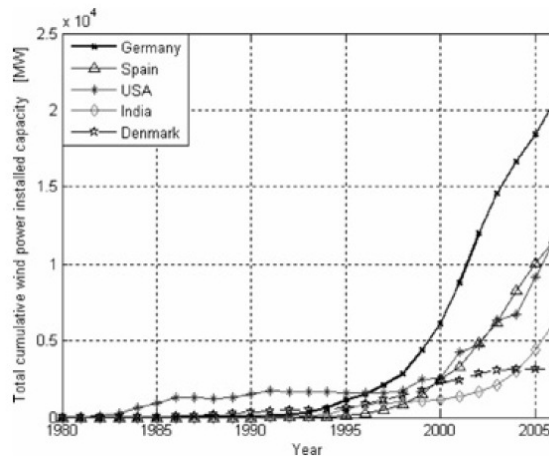


Fig. 1. Total cumulative wind power installed capacity for different countries (1980–2006)

The energy production can be increased by 2–6% for a variable-speed wind turbine in comparison to a fixed-speed wind turbine, while in it is stated that the increase in energy can be 39% [3]. The gain in energy generation of the variable-speed wind turbine compared to the most simple fixed-speed wind turbine can vary between 3–28% depending on the site conditions and design parameters. Efficiency calculations of the DFIG system have been presented in several papers [3]. A comparison to other electrical systems for wind turbines are, however, harder to find. One exception presented is in [3], where Datta et al. have made a comparison of the energy capture for various WT systems. The energy capture can be significantly increased by using a DFIG. They state an increased energy capture of a DFIG by over 20% with respect to a variable-speed system using a cage-bar induction machine and by over 60% in comparison to a fixed-speed system. One of the reasons for the various results is that the assumptions used vary from investigation to investigation. Factors such as speed control of variable-speed WTs, blade design, what kind of power that should be used as a common basis for comparison, selection of maximum speed of the WT, selected blade profile, missing facts regarding the base assumptions etc, affect the outcome of the investigations. There is thus a need to clarify what kind of energy capture gain there could be when using a DFIG WT, both compared to another variable-speed WT and towards a traditional fixed-speed WT [3].

3. DFIG discription

Doubly-fed induction generators (DFIGs) are widely used in wind power systems. A DFIG works as a component of a wind power system, as shown below, where the wind turbine transforms wind energy into mechanical energy, and the DFIG transforms mechanical energy into electrical energy. For a DFIG, both the stator and the rotor are equipped with poly-phase AC windings. The stator and rotor windings may, or may not, have the same number of phases, but they must have the same number of poles p [9].

A DFIG system can deliver power to the grid through the stator and rotor, while the rotor can also absorb power. This depends on the rotational speed of the generator. If the generator operates above synchronous speed, power will be delivered from the rotor through the converters to the network, and if the generator operates below synchronous speed, then the rotor will absorb power from the network through the converters [1].

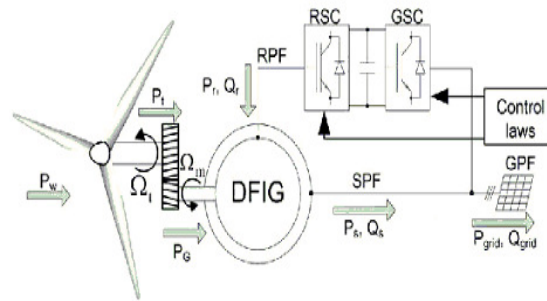


Fig. 2. Typical configuration of a DFIG wind turbine

In order to produce terminal voltages with desired frequency f in the stator winding, the rotor winding must be excited by balanced poly-phase currents with the slip frequency Sf via an AC-DC-AC convert. Slip s is defined as [9]:

$$s = 1 - n / n_0 \quad (1)$$

Where n is the rotor speed, and n_0 is the synchronous speed as given below:

$$n_0 = 60 f / p \quad (2)$$

When the rotor speed is lower than the synchronous speed, the rotor currents have the same phase sequence as the stator currents, and the rotor winding gets power from the converter. However, when the rotor speed is higher than the synchronous speed, the phase sequence of the rotor currents is different from that of the stator currents, and the rotor winding outputs power to the converter [1-9].

For a given wind turbine, the power coefficient (the ratio of turbine power to the wind power), is a function of the tip speed ratio (the ratio of the blade tip speed to the wind speed). In order to track the maximum power point, the tip speed ratio must keep constant - at its optimal value. The input mechanical power with Maximum Power Point Tracking (MPPT) must satisfy [9]:

$$P_{mech} = P_{m_ref} (\omega_m / \omega_{ref})^3 \quad (3)$$

Where P_{m_ref} is the turbine power with MPPT at a reference speed of ω_{ref} based on the optimal tip speed ratio, and ω_m is the rotor speed in rad/s. The rotor mechanical loss is:

$$P_f = P_{f_ref} (\omega_m / \omega_{ref})^3 \quad (4)$$

Where P_{f_ref} is mechanical loss measured at a reference speed of ω_{ref} . The electromagnetic power in the air gap is:

$$P_{em} = (P_{mech} - P_f) / (1 - s) \quad (5)$$

Therefore, the stator output electrical power at rated operation is:

$$P_1 = P_{em} - m_1 I_1^2 R_1 = m_1 V_1 I_1 \cos \varphi \quad (6)$$

where m_1 is the number of phases of the stator winding, R_1 is the stator phase resistance, V_1 is the stator rated phase voltage, I_1 is the rated stator phase current to be determined, and $\cos \varphi$ is the rated power factor. Solving for I_1 , one obtains:

$$I_1 = \frac{2 P_{em} / m_1}{V_1 \cos \varphi + \sqrt{(V_1 \cos \varphi)^2 + 4 R_1 P_{em} / m_1}} \quad (7)$$

Then, based on the equivalent circuit shown below, one obtains:

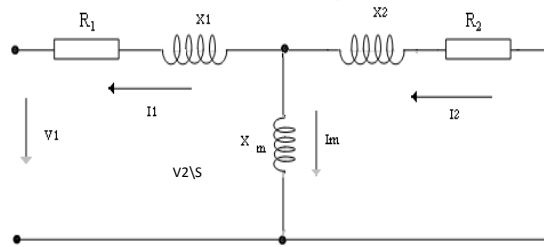


Fig. 3. DFIG equivalent circuit

Now, rotor input electrical power can be computed as:

$$P_2 = s P_{em} + m_2 I_2^2 R_2 \quad (8)$$

Where m_2 is the number of phases of the rotor winding.

The electromagnetic torque T_{em} is:

$$T_{em} = P_{em} / \omega \quad (9)$$

Where ω denotes the synchronous speed in rad/s.

The input mechanical torque on the shaft is:

$$T_{mech} = T_{em} + T_f \quad (10)$$

Where T_f denotes the frictional torque.

The total electrical output power is:

$$P_{elec} = P_1 - P_2 - P_{Fe} \quad (11)$$

Where p_{Fe} is the core loss. The efficiency is defined as:

$$\eta = \frac{P_{elec}}{P_{mech}} 100 \% \quad (12)$$

4. Geometric Dimension And Parameters Design Of Dfig Studie

The operation principle of electric machines is based on the interaction between the magnetic fields and the currents flowing in the windings of the machine. Rotational Machine Expert (RMxprt) is an interactive software package used for designing and analyzing electrical machines, is a module of Ansoft Maxwell 12.1 [10]. The structure of coil connection is shown in Fig. 4, Fig. 5, and the 3D geometries of the generator are shown in Fig. 6

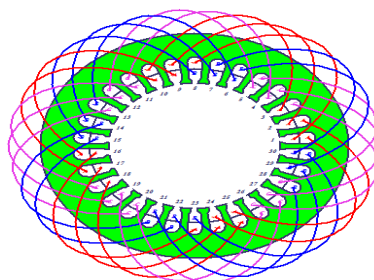


Fig. 4. Stator and coil structure of the designed generator

Table 1. Stator and rotor slot parameters

Stator Slot Parameter	Rotor Slots Parameter
hs0 (mm): 2	hr0 (mm): 2
hs1 (mm): 2	hr1 (mm): 2
hs2 (mm): 10	hr2 (mm): 15
bs0 (mm): 2.5	br0 (mm): 2.5
bs1 (mm): 8.52819	br1 (mm): 9.19419
bs2 (mm): 10.6303	br2 (mm): 5.24462
rs (mm) : 2	rr (mm) : 2

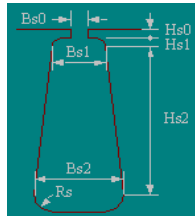


Fig. 5. Slot type

Table 2. SOME RATED VALUES, GEOMETRIC PARAMETERS OF THE DESIGNED MACHINES

Somme Electrical And Dimensional Parameters	Value
Rated output power (kW)	0.55
Rated voltage (V)	220
Given rated speed (rpm)	1500
Number of poles	4
Outer diameter of stator (mm)	180
Inner diameter of stator (mm)	121
Number of stator slots	30
Outer diameter of rotor (mm)	120
Inner diameter of rotor (mm)	50
Number of stator slots	24
Length of stator core (rotor) (mm)	65
Stacking factor of stator core	0.97
Stacking factor of iron core	0.97
Frictional loss (W)	12
Operating temperature (^o C)	75

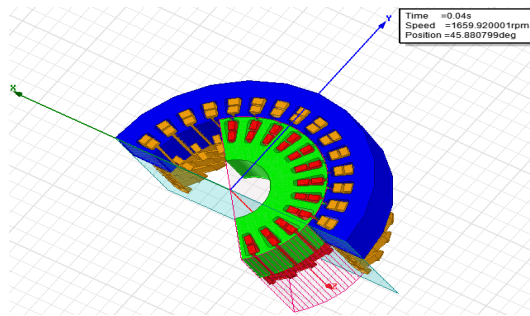


Fig. 6. 3D view of the DFIG inner rotor designed

5. Simulation Results

The finite element model is created. First, the geometric outlines are drawn, which is similar to the available mechanical engineering packages. Then, material properties are assigned to the various regions of the model. Next, the current sources and the boundary conditions are applied to the model. Finally, the finite element mesh is created. In the solver part, the finite element solution is conducted [10]. The FEA model of electromagnetic field is built by Maxwell12D; in this case the total number of mesh element is 9336.

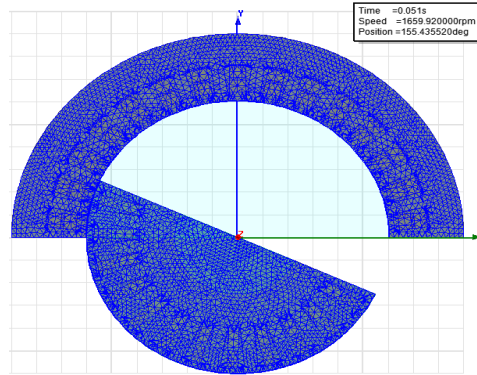
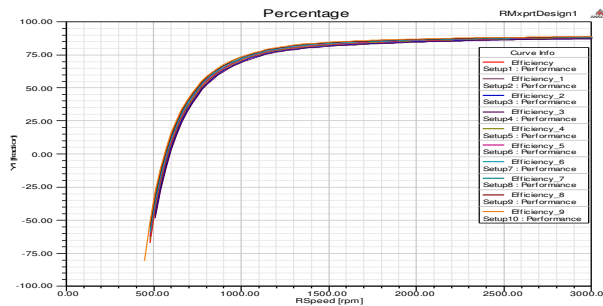


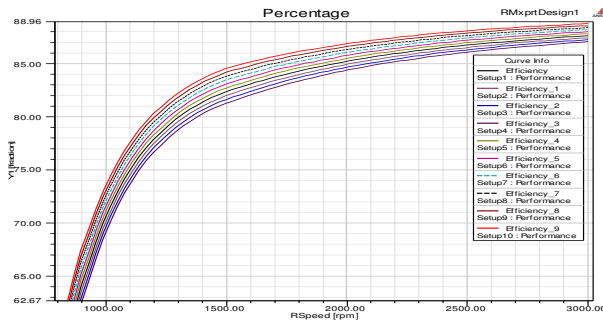
Fig. 7. 2D DFIG inner rotor mesh

A. Efficiency of DFIG at variable environmental thermal condition

The DFIG performance is obtained, by considering a variable ambient temperature, Fig 8. Show the influences of environmental thermal condition on efficiency, the increase in the ambient temperature, so the DFIG losses increase, thus the efficiency decreases.



a. Percentage (efficiency) variation at different thermal condition



b. ZOOM

Fig. 8. Percentage (efficiency) variation at different thermal condition

B. DFIG modelisation results by 2D finite element method

One considers a DFIG connected an infinite bus, the grid frequency is 50Hz, and turns at constant speed 1660rpm.

Fig. 9 show the torque variation, the torque value in steady state is -3.5 Nm.

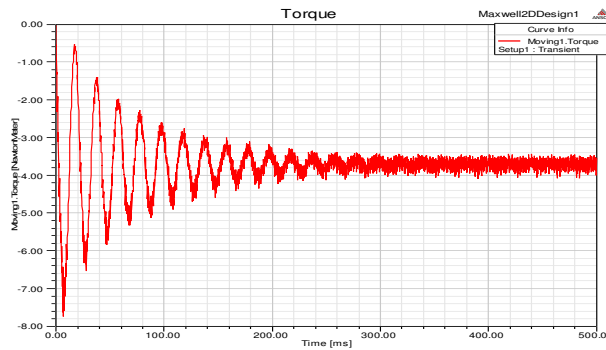


Fig. 9. Torque in DFIG inner rotors

Fig. 10 illustrates the stator and rotor flux linkage of DFIG, when in study state the first one value is 0.6wb and the second is 0.2wb.

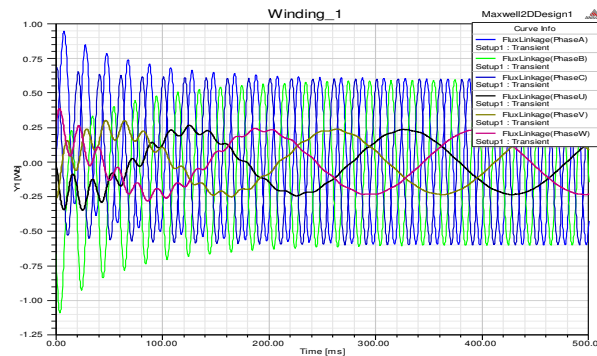


Fig. 10. DFIG stator and rotor flux linkage

The DFIG stator current winding is shown in Fig. 11, the magnitude is 2A and the frequency is 50Hz, The frequency equal has 50 Hz by what the speed (mechanical) east notes.

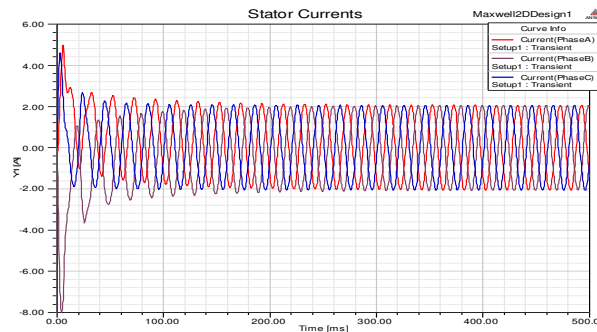


Fig. 11. DFIG stator current winding

There are two types of stranded loss quantities, StrandedLoss and StrandedLossR [9]:

- StrandedLoss represents the resistive loss in a 2D or 3D volume and is calculated by:

$$Solid Loss = \frac{1}{\sigma} \int J^2 \quad (13)$$

Where J is the conductivity of the material.

•StrandedLossR represents the loss based on I2 times the resistance R.

Fig. 12 illustrates the two types of loss, when the value of StrandedLoss in transient state is 355w and stabilized at 24w in steady-state, but the StrandedLossR is constant at 14.3w.

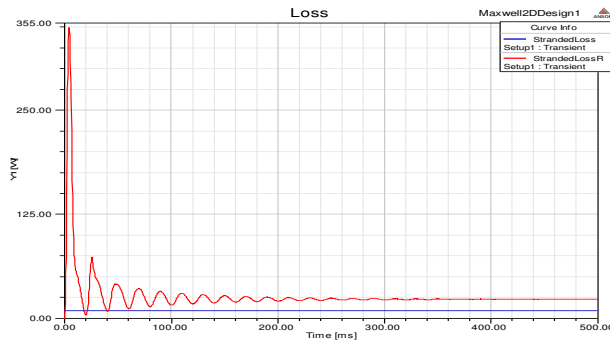


Fig. 12. DFIG StrandedLoss and StrandedLossR

Fig. 13 shows the DFIG stator and rotor induced voltage, when the value of stator is 185v, but the value of rotor induced voltage is 8v.

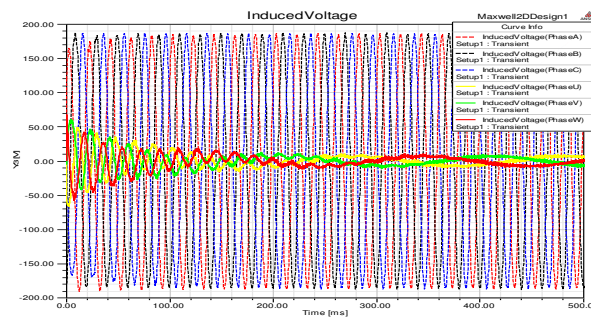


Fig. 13. DFIG stator and rotor induced voltage

Fig.14 show DFIG stator winding current spectrum, one does not find the harmonic by that the current operate and purely sinusoidal.

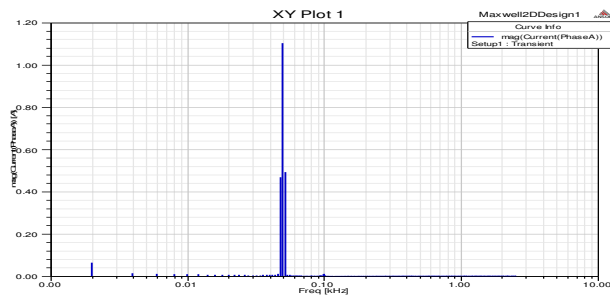


Fig. 14. DFIG stator winding current spectrum

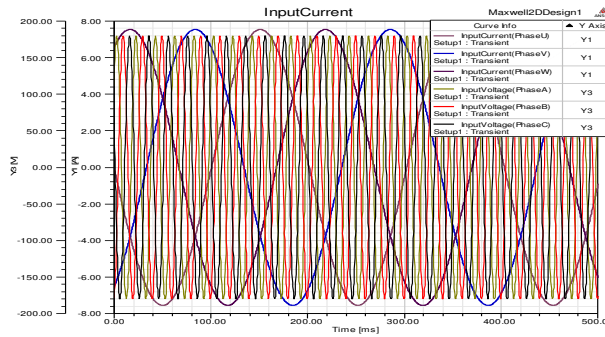


Fig. 15. Rotor current and stator voltage of DFIG

Fig. 15 shows the rotor current and stator voltage of DFIG, the magnitude and the frequency of the first one is 9.5A is ≈ 5 Hz, and the second one is 180v is 50Hz respectively.

C. Field results in 2D of the elemnt finits model

The FEA model of electromagnetic field is built by Maxwell2D, the flux, flux density, field intensity.

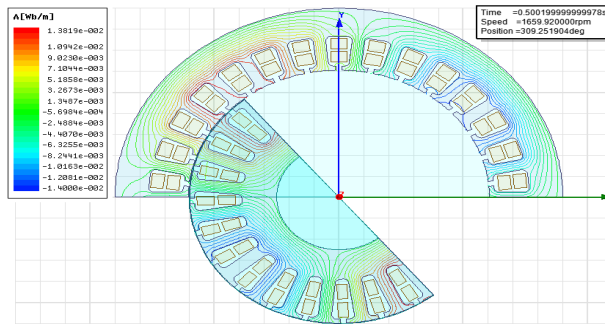


Fig. 16. Flux distribution of DFIG at 0.5s

The Fig.16 indicates the flux line distribution of the DFIG at 0.5s.

It is important to note that in order to obtain accurate results, the triangular mesh elements assigned to the airgap should have an aspect ratio close to one. A large aspect ratio between the sides of a triangular element will result in accurate computation of the flux density and hence the electromagnetic torque.

Fig 17 shows the DFIG’s flux density distribution at 0.5s, the maximum value of flux density is 1.47T.

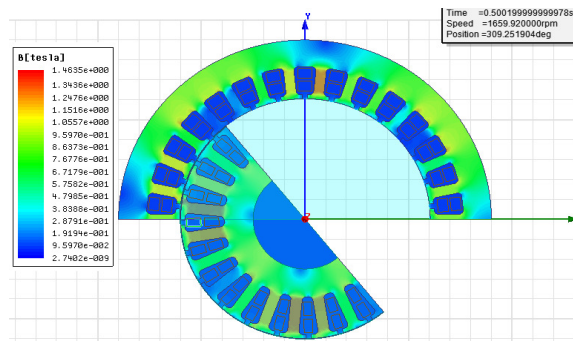


Fig. 17. flux density of DFIG at 0.5s

Fig.18 indicates the vector diagram and contours diagram of flux density at 0.5s.

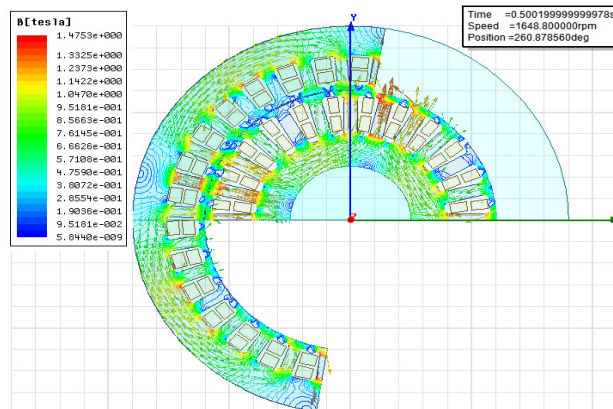


Fig. 18. Contours and vector diagrams of flux density in DFIG

According to Fig. 18 and Fig. 16, the flux line and magnetic field are symmetrical in the whole machine and the distribution regularities of flux line and magnetic field are the same.

The total loss of DFIG is illustrated in fig19, when the winding losses have a great contribution.

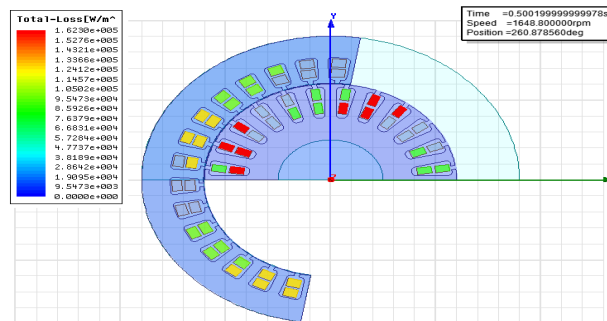


Fig. 19. Total Loss of DFIG

D. Field results in 3D of the finite element model

The 3D FEA model of electromagnetic field is built by Maxwell 3D, this simulation is obtained by Terra pc (QuadroFX380, i7 CPU, 3.07 GHZ, 8 CPU and 4G RAM). Our model of DFIG used in Maxwell 3D environment has 98586 number of mesh element. The largest saving in computation time is made by doing the simulation in 2D instead of 3D. The analyze will be fairly limited due to the large increase in simulation time, approximately 4 minutes per time step compared to 5 seconds for a corresponding 2D model. In our application the simulation rest in execution during some day.

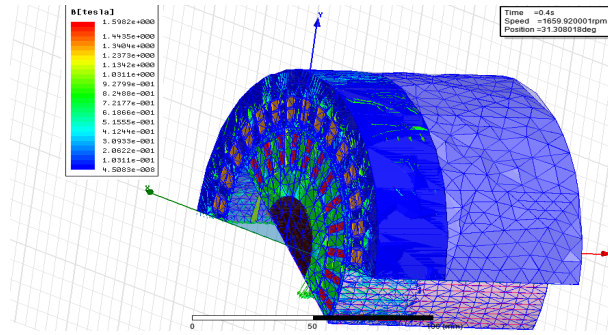


Fig. 20. 3D DFIG inner rotor mesh

Fig 20 shows the 3D DFIG's flux density distribution at 0.4s, the maximum value of flux density is 1.59T. According to Fig. 17 and Fig. 21, the maximum value of flux density obtained by 3D model is bigger than in 2D,

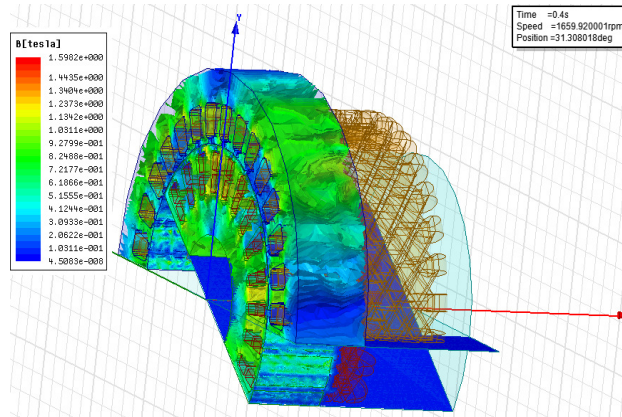


Fig. 21. 3D flux density of DFIG at 0.4s

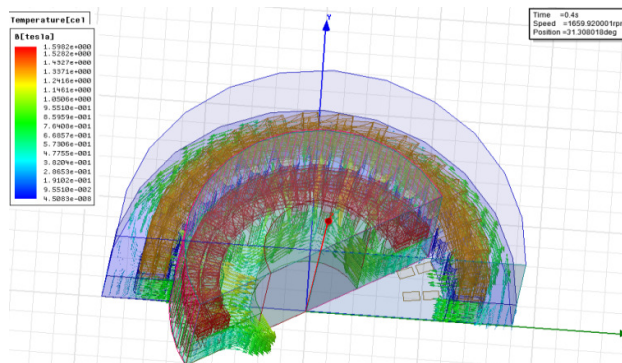


Fig. 22. 3D vector diagram of flux density of DFIG at 0.4s

Fig.23 indicates the 3D vector diagram of flux density at 0.4s.

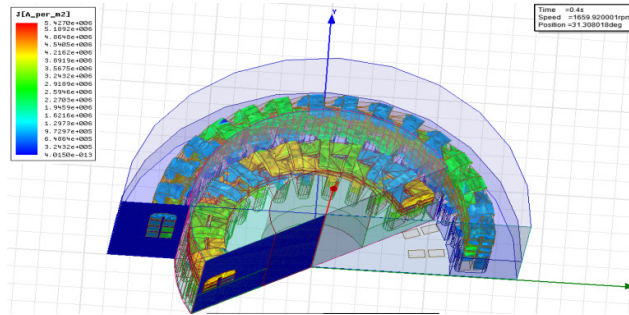


Fig. 23. 3D current density of DFIG at 0.4s

Fig.24 shows the 3D total loss of DFIG at 0.4s.

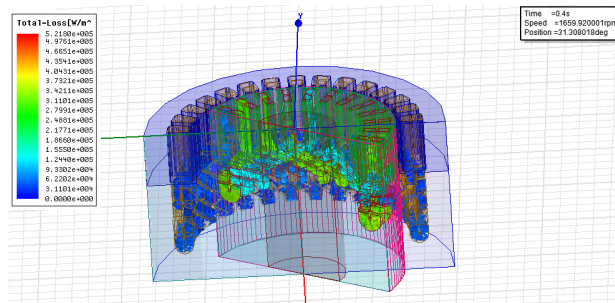


Fig. 24. 3D Total loss of DFIG inner rotor

6. Conclusion

Finite element analysis (FEA) is a frequently used method for analysis of electromechanical converters. As a numerical analysis method, FEA allows for including any practical material, external excitation (voltage driven or current driven), inclusion of motion, and nonlinear effects such as magnetic saturation and eddy current effects.

A 2D model of the DFIG inner rotor is given, solved, some simulation result is given and commented, to return our simulation results finer a 3D model is developed and solved, but the resolution time is very large, this time is a scale of the days.

This model 2D and 3D obtained by using Ansoft finite element software, this last can be used as an effective way to design and calculate the DFIG performance. This work is the necessary preparations for design and development high reliability and high security of DFIG applications.

References

- [1] AL. Olimpo, J. Nick, E. Janaka, C. Phill and H Mike, Wind Energy Generation Modelling and Control, John Wiley & Sons, Ltd 2009.
- [2] Ian woofenden, wind power for dummies, Wiley Publishing, 2009.
- [3] A. Petersson, Analysis, Modeling and Control of Doubly-Fed Induction Generators for Wind Turbines, phd thesis, chalmers university of technology, GÖteborg, Sweden 2005.
- [4] Martin O. L. Hansen, Aerodynamics of Wind Turbines, Earthscan in the UK and USA in 2008.
- [5] Zongxi Fang ,Permanent magnet machine topologies for wind power generation, university of Sheffield 2010.

- [6] B.C. Pal F. Mei, Modelling adequacy of the doubly fed induction generator for small-signal stability studies in power systems, IET Renewable Power Generation 2008.
- [7] H. Li, Z. Chen, Overview of different wind generator systems and their comparisons, Renewable Power Generation, IET 2007.
- [8] H. Li1, Z. Chen, Henk Polinder, research report on models for numerical evaluation of variable speed different wind generator systems, Integrating and strengthening the European Research Area, 2002-2006.
- [9] Help of Ansoft Maxwell V12®, Ansoft Corporation 2010.
- [10] H. Mellah, K.E Hemsas, Dynamic design and simulation analysis of permanent magnet motor in different scenario of fed alimentation, conference international on automatique and mécatronique, novembre 22 -23, 2011, usto, oran, Algeria.